

See discussions, stats, and author profiles for this publication at: <https://www.researchgate.net/publication/231627180>

pH-Dependent Appearance of Chiral Structure in a Langmuir Monolayer

ARTICLE in THE JOURNAL OF PHYSICAL CHEMISTRY B · MAY 2000

Impact Factor: 3.3 · DOI: 10.1021/jp0006375

CITATIONS

25

READS

30

7 AUTHORS, INCLUDING:



Alokmay Datta

Saha Institute of Nuclear Physics

123 PUBLICATIONS 1,112 CITATIONS

SEE PROFILE



Chung-Jong Yu

Pohang University of Science and Technology

53 PUBLICATIONS 750 CITATIONS

SEE PROFILE



Andrew G. Richter

Valparaiso University (USA)

56 PUBLICATIONS 991 CITATIONS

SEE PROFILE



Jianming Bai

Brookhaven National Laboratory

138 PUBLICATIONS 2,230 CITATIONS

SEE PROFILE

pH-Dependent Appearance of Chiral Structure in a Langmuir Monolayer

A. Datta,[†] J. Kmetko,^{*,†} C.-J. Yu,[†] A. G. Richter,[†] K.-S. Chung,[‡] J.-M. Bai,[‡] and P. Dutta[†]

Department of Physics and Astronomy, Northwestern University, Evanston, Illinois 60208-3112, and Metals & Ceramics Division, Oak Ridge National Laboratory, Oak Ridge, Tennessee 37830

Received: February 18, 2000; In Final Form: April 13, 2000

Grazing incidence X-ray diffraction studies on a heneicosanoic (C_{21}) acid monolayer with cadmium ions in the subphase, at near-zero surface pressure and $\sim 9^\circ\text{C}$, show that there exists a pH “window” within which the monolayer takes on a chiral structure and an ordered superlattice is also observed. Below this pH window, the monolayer has a tilted structure like that of a pure fatty acid monolayer at low pressures, indicating negligible headgroup–ion interaction. Above the window, the monolayer goes to a structure very similar to the high-pressure untilted S phase seen in pure fatty acid monolayers. The chiral structure is never seen when cadmium is replaced by zinc, another divalent metal with only slightly lower electronegativity, or (as reported earlier) with calcium. Raising temperature within the cadmium pH window destroys the superlattice and takes the monolayer to the backbone-disordered Rotator-I structure.

Introduction

The mechanical properties of a Langmuir monolayer of long-chain fatty acid molecules are changed by the presence of divalent metallic cations in the aqueous subphase. This has been known for some time, and it is also known that the presence of such ions improves transfer of Langmuir–Blodgett (LB) films from the Langmuir monolayer and enhances the crystalline order in those LB films.^{1,5} It is therefore worthwhile to learn more about the nature of headgroup interactions in monolayers and how they are affected by metallic cations.

The role of metal ions has been extensively studied in organic films at air–solid interfaces (i.e., in LB films) as well as at the air–water interface.^{1–5} The area per molecular headgroup of the specific fatty acid salt at the solid interface has been correlated with Pauling’s electronegativity of the corresponding counterion, and a determination of the degree of the covalent or ionic nature of the bond has been made.² Surface potential measurements on monolayers at the air–water interface³ showed that the alkaline earth metals (Ba, Ca, and Mg) make electrostatic bonds with the headgroups and Pb, Cd, and Co interact by covalent bonding. In an infrared reflection–absorption spectrometry on Langmuir monolayers,⁴ Cd and Pb induced a formation of more ordered structures than Ca did. This effect was again explained by varying degree of ionic or covalent bonding: covalent for Cd and Pb and ionic for Ca.

The effect of divalent metal ions on Langmuir monolayers was also recently studied with grazing incidence diffraction (GID) of synchrotron X-rays. This study⁶ divided the interactions into two categories. The first kind of interaction produces high-pressure monolayer phases at low surface pressure, i.e., creates an “effective high pressure” by attracting the headgroups closer together. As this phenomenon has been observed with electrostatic metals such as calcium,⁷ a radially symmetric screened Coulomb type interaction is assumed to be involved.⁸ The second category of headgroup–ion forces is seen with more

electronegative ions such as cadmium.⁹ This interaction produces an entirely new phase with an asymmetrically distorted, i.e., chiral lattice of the monolayer. More interestingly, it also produces a number of weak diffraction peaks that have been indexed as a supercell of the monolayer lattice. This superlattice is claimed to be due to a monolayer of cadmium or, as suggested by reflectivity data,⁹ CdOH^+ ions forming a two-dimensional lattice. The formation of this new structure is presumed to be due to an anisotropic, polar-bond forming interaction between a weak acid and an electronegative metal ion.

However, the correlation between headgroup–ion interaction and monolayer phase structure is not well understood. Questions remain as to whether such clear categories of Coulomb versus covalent bonding interactions do exist and, even if they do, whether a system can be tuned to pass from one to the other. An answer to the first question requires comparative studies of various divalent metals with different values of Pauling electronegativity, especially ones that are close in the electronegativity values. The second involves a way to tune headgroup–ion interaction for the same ion, and the easiest way available is to change the subphase pH.

In this paper, we present results of systematic GID studies of heneicosanoic acid ($\text{COOH}(\text{CH}_2)_{19}\text{CH}_3$, C_{21} acid) monolayers. The structures of different phases of these monolayers at close to zero surface pressure have been studied with cadmium and zinc, two different divalent metal cations with close values of electronegativity in the subphase, and with variations in subphase pH and temperature.

Experiment

GID studies were performed at the Beam Line X-14 (Oak Ridge National Laboratory Beam Line) of the National Synchrotron Light Source, Brookhaven National Laboratory. This is a bending-magnet beam line. A description of the experimental setup has been given previously.¹⁰ The X-ray beam of energy 8.0 keV was focused to a vertical width of 800 μm and was horizontally unfocused (horizontal width ~ 17 mm). This beam was then reflected from a platinum coated mirror so as to be incident at an angle of ~ 1.8 mrad to the water surface,

* Author for correspondence. Phone: 1-847-491-3477. Fax: 1-847-491-9982. E-mail: j-kmetko@nwu.edu.

[†] Northwestern University.

[‡] Oak Ridge National Laboratory.

just below the critical angle for total external reflection from water, to reduce background scattering. The detector was scanned horizontally to measure the in-plane component of the resultant wave vector (or momentum transfer vector) K_{xy} and vertically to measure vertical component K_z . As Langmuir monolayers are powders in the plane the in-plane wave vector cannot be decomposed further into the x and y components. The total momentum transfer lies in a plane normal to the hydrocarbon chains and, hence, if chains are tilted to the water surface some or all of the diffraction peaks will have maximum intensity at nonzero K_z . Vertical and horizontal soller slits in front of the detector defined a horizontal resolution of $\sim 0.01 \text{ \AA}^{-1}$ full width at half-maximum (fwhm) for K_{xy} scans and a vertical resolution of $\sim 0.05 \text{ \AA}^{-1}$ fwhm for K_z scans. Two scintillation detectors were used to monitor the intensities of the beam incident on (beam monitor) and specularly reflected (height monitor) from the water surface. All data are presented after subtracting a linear background.

Water purified to $18 \text{ M}\Omega\text{-cm}$ resistivity by a Barnstead Nanopure II system was used to prepare the subphase. Heneicosanoic (C21) acid (Sigma, quoted purity 99%) was chosen as the amphiphile because the phase diagram of pure C21 acid is well-known⁸ and could readily be compared to estimate the effect of ions. Chloroform (Aldrich, quoted purity 99.9+%) was the spreading solvent and sodium hydroxide (NaOH, Aldrich, quoted purity 99.99%) was used to raise the pH. The salts zinc acetate ($\text{Zn}(\text{Ac})_2$, Aldrich, quoted purity 99.999%) and cadmium chloride (CdCl_2 , Aldrich, quoted purity 99.99+%) were used to produce the ions in the aqueous subphase. All chemicals were used without further purification.

About $65 \text{ }\mu\text{L}$ of a 0.87 mg/mL solution of C21 acid in chloroform was spread. Solutions of the barium and zinc salts with $5 \times 10^{-4} \text{ M}$ concentration and solutions of the cadmium salt with 10^{-4} M concentration were used as subphases. Temperature was varied from 9 to $22 \text{ }^\circ\text{C}$ ($\pm 0.1 \text{ }^\circ\text{C}$) and the pH from 6 to $9.2 (\pm 0.1)$. A new monolayer was used for each set of pH and surface pressure measurements. It was allowed to remain at a steady temperature for about 40 min and then compressed to a very small positive surface pressure which will be quoted as $\sim 0 \text{ dyn/cm}$. Surface pressure (π) was measured with $\pm 0.5 \text{ dyn/cm}$ accuracy (Balance ST9000, Nima Technology). A slight overpressure of helium was maintained in the trough to reduce radiation damage and air scattering. The monolayers still sustained radiation damage, however, and reproducible data were obtained only during the first 2 h of X-ray exposure.

Results

1. Variations with pH and Temperature. We performed a check of consistency with the results of previous studies⁹ (using monolayers of $\text{COOH}(\text{CH}_2)_{18}\text{CH}_3$, referred to here as C₂₀ acid, with 10^{-3} M CdCl_2 in subphase, pH raised to 8.85 with ammonium hydroxide, at $9 \text{ }^\circ\text{C}$) as a necessary first step. Unfortunately, we could not reproduce the previously published results with C₂₁ acid using the same CdCl_2 concentration, with the pH raised to the prescribed value either with ammonium or sodium hydroxide, anywhere between 7 and $12 \text{ }^\circ\text{C}$, but obtained a single, broad peak only. On the other hand, we could reproduce those results very closely when the concentration of the ions was 10^{-4} M , and we found that raising the pH by sodium or ammonium hydroxide gives identical diffraction patterns. We have therefore used this lower concentration for all measurements on CdCl_2 reported here, and used NaOH throughout to raise pH.

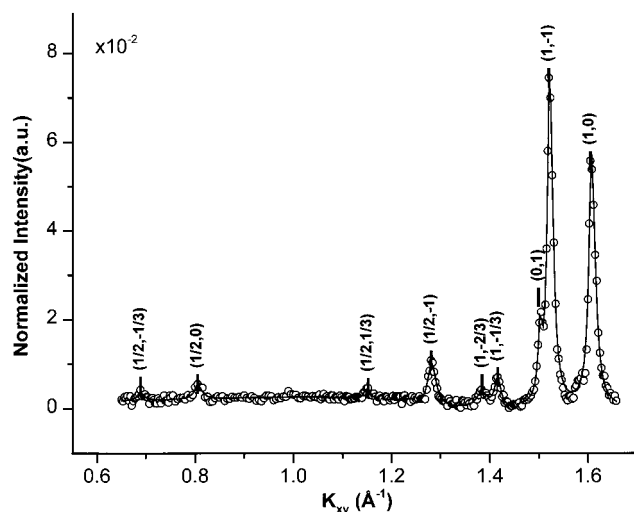


Figure 1. Normalized diffracted intensity (arbitrary units) versus K_{xy} , the in-plane component of momentum transfer vector (\AA^{-1}), for a heneicosanoic acid Langmuir monolayer at $\sim 9.2 \text{ }^\circ\text{C}$ and $\sim 0 \text{ dyn/cm}$ surface pressure, with 10^{-4} M CdCl_2 in the subphase and pH raised to 8.5 with NaOH. Data taken at $K_z = 0$. Peaks are indexed following the assignment described in text. These data are essentially identical to those reported in ref 9.

TABLE 1: Variation of Structural Parameters with pH and Temperature^a

T ($^\circ\text{C}$)	pH	a (\AA)	b (\AA)	A (\AA^2)	A' (\AA^2)	ξ	θ (deg)	ϕ
9.2	6.2	8.70	4.83	21.02	19.45	0.04	22	NN
9.2	8.5	7.77	4.89	19.00	18.75	0.09	8	$\sim\text{NNN}$
9.2	9.3	7.45	5.00	18.64	18.64	0.15	0	
18.0	8.5	7.83	4.86	19.02	19.02	0.07	0	
22.0	8.5	7.99	4.80	19.18	19.18	0.04	0	

^a For C21 acid monolayer spread on CdCl_2 (10^{-4} M) in subphase at $\sim 0 \text{ dyn/cm}$ surface pressure. The lattice parameters a and b refer to a centered rectangular cell with two molecules per unit cell. A designates the area per molecule in the horizontal plane (area per headgroup) and A' designates the area per molecule in the plane normal to the hydrocarbon chains (area per chain). The distortion magnitude ξ is defined in ref (see text), θ is the tilt angle, and ϕ is the tilt azimuth (NN = nearest and NNN = next nearest neighbor).

The diffraction pattern was essentially invariant over a pH range of ~ 7 to ~ 9 . In Figure 1 we show a typical wide K_{xy} scan taken at $K_z = 0$ for a pH value of 8.5. We see the strong triplet in the K_{xy} range of $1.45\text{--}1.70 \text{ \AA}^{-1}$ and the weak peaks at lower values of K_{xy} ($0.65\text{--}1.45 \text{ \AA}^{-1}$), just as has been reported with C₂₀ acid.⁷ Our assignment of $\{h, k\}$ indices to the K_{xy} positions of these peaks follows that of ref 9 and are indicated in Figure 1. The primitive unit cell is oblique (corresponding to an asymmetrically distorted hexagonal or chiral lattice) with lattice parameters $a' = 4.56 \text{ \AA}$, $b' = 4.89 \text{ \AA}$, and $\gamma = 121.6^\circ$, while the peaks with the fractional indices gave a 2×3 superlattice of this oblique cell. Since two peaks of the triplet are nearly degenerate, we could determine an equivalent centered pseudo-rectangular unit cell (with two molecules per unit cell) through the transformations, $a = 2a' + b'$, $b = b'$. The values of the lattice parameters a , b , and A , the area per molecule in the horizontal plane (water surface) are given in Table 1. Since the headgroups always lie on this plane, A is the area per headgroup. The angle between a and b is 89.2° .

In Figure 2a we show the intensity contours of a typical weak diffraction peak ('superlattice peak') from the scan of Figure 1 as a function of K_{xy} and K_z , while Figure 2b shows the contours for the strong triplet from the same scan. It is seen that the superlattice peak has its maximum at $K_z = 0$. Except for the

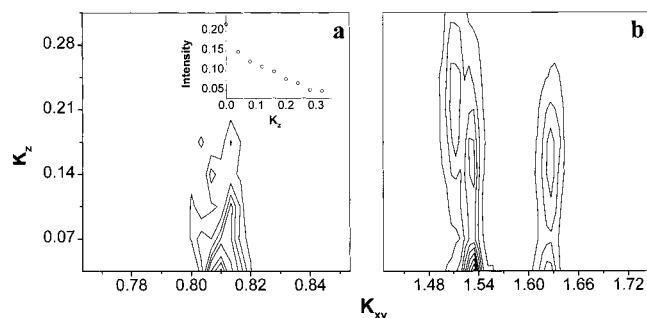


Figure 2. Intensity contours (arbitrary units) in the K_z/K_{xy} plane for the monolayer described in Figure 1: (a) a weak superlattice peak and (b) a strong triplet. K_z profile (Bragg rod) at the superlattice peak is shown in the inset.

contribution due to refraction close to the water surface from the maxima of the Vineyard function¹¹ at and near $K_z = 0$, all three peaks of the triplet are out-of-plane and all have sharp K_z maxima. Fits of the K_{xy} peaks with Lorentzian functions and the K_z peaks with Gaussian functions¹² gave the peak positions and widths. The peak positions were then used to obtain the tilt θ of the hydrocarbon chains from the vertical, the azimuth ϕ of the tilt, the area A' per molecule in the plane normal to the chains, and ξ the distortion magnitude, following Kaganer et al.,¹³ where $\xi = (\alpha^2 - \beta^2)/(\alpha^2 + \beta^2)$, α and β being respectively the major and minor axes of the ellipse that passes through all six nearest neighbors of a given molecule. These values are given in Table 1. The chains are found to be tilted almost along the longer (b) axis of the centered pseudo-rectangular unit cell, as also observed with C_{20} acid.⁹ The amount of tilt, however, is less in C_{21} acid (it was about 11° for C_{20} acid).

From fwhm's of the K_z peaks fitted with a Gaussian function, we obtained, using Scherrer's formula, an estimate of the thickness of the monolayer corresponding to the K_z profile (thickness = $0.9 \times 2\pi/\text{fwhm}$).⁸ For the triplet peaks, the thickness comes out to be ~ 29 Å, consistent with the d -spacing in bulk crystals of fatty acid cadmium salts,¹⁴ while the "superlattice peak" (K_z profile along the K_{xy} peak shown in Figure 2a (inset)) appears to come from a layer of thickness ~ 10 Å, which is about 4 times thicker than estimated for a monolayer of CdOH^+ .

Below and above the pH window 7–9, the monolayer underwent major structural changes as reflected in the three in-plane ($K_z = 0$) scans shown in Figure 3. All scans were performed at 9.2°C with CdCl_2 (10^{-4} M) in the subphase. Figure 3 (top) depicts the K_{xy} scan when no NaOH was added to the subphase to raise the pH. The pH of this subphase was measured to be ~ 6.2 , i.e., below the pH window. No superlattice peaks were observed. The K_z/K_{xy} contour plot of the scanned region in Figure 3 (top) is shown in Figure 4a. It shows an in-plane and an out-of-plane peak, and by fitting these peaks to obtain the K_z and K_{xy} positions we found the structural parameters for this phase (see Table 1). There is a centered rectangular unit cell (with two molecules per unit cell) with chains tilted toward a nearest neighbor by an angle of about 22.3° from the vertical. The lattice spacings are almost identical to those of the L_2 phase seen previously in monolayers of the pure acid.¹² This indicates that there is negligible interaction between the headgroups and the ions below the pH window.

Figure 3 (middle) shows the monolayer within the window and we have already discussed the structure of this phase with its pseudo-rectangular cell and superlattice peaks (not shown in this figure). Figure 3 (bottom) shows the diffraction pattern from the monolayer above the window (pH ~ 9.3). Only two

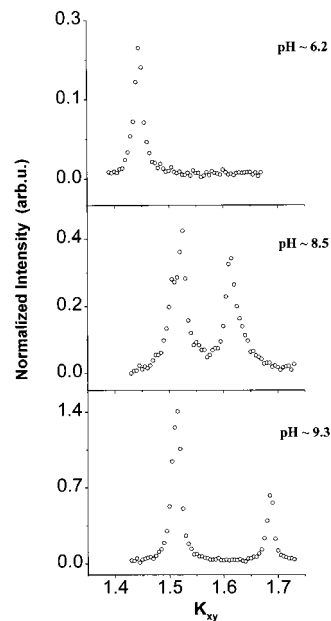


Figure 3. Normalized diffracted intensity (arbitrary units) versus K_{xy} for a heneicosanoic acid Langmuir monolayer at $\sim 9.2^\circ\text{C}$ and ~ 0 dyn/cm surface pressure, with 10^{-4} M CdCl_2 in the subphase and different values of pH. Data taken at $K_z = 0$.

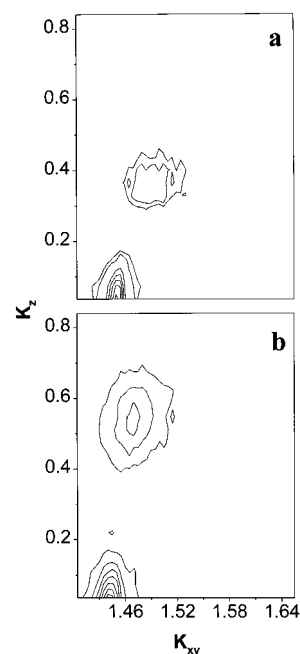


Figure 4. Intensity contours (arbitrary units) in the K_z/K_{xy} plane for (a) the monolayer described in Figure 3 (top), pH ~ 6.2 , and (b) a heneicosanoic acid monolayer with no divalent ions in the subphase but with pH raised to 9.3 by NaOH.

peaks were observed between 0.65 and 1.7 Å⁻¹ in K_{xy} which are shown in the scan. Both peaks were found to be in-plane, i.e., with maximum intensity at $K_z = 0$. Structural parameters are given in Table 1. This is again a centered rectangular unit cell (with two molecules per unit cell) with untilted chains which is very similar to the S phase observed in monolayers of pure C_{21} acid at the same temperature but at a much higher pressure of > 30 dyn/cm.¹⁵ This similarity indicates an isotropic attractive force due to the divalent ions that compresses the organic monolayer.

To check out the possibility that, at high values of subphase pH, the change in structure is due to the sodium hydroxide used

to raise the pH rather than to any change in the headgroup–cadmium ion interactions, we performed diffraction scans on a C₂₁ acid monolayer with no CdCl₂ in the subphase but the pH raised to 9.3 by NaOH, at 9.2 °C and ~ 0 dyn/cm surface pressure. Figure 4b shows the K_z/K_{xy} contour plot of the two peaks observed. They are almost identical to those in Figure 4. From an analysis of the peaks in Figure 4b we obtained a centered rectangular lattice for the monolayer (two molecules per unit cell) with $a = 8.75$ Å, $b = 4.92$ Å, $A = 21.50$ Å², the chains tilted toward nearest neighbors by an angle of 21.9° from the vertical, and $A' = 19.95$ Å², which are very similar to what was found for the monolayer with CdCl₂ in the subphase but no NaOH (Figure 4a and Table 1). We have already seen that the structure is similar to that of a pure C₂₁ acid monolayer at ~ 10 °C and ~ 0 dyn/cm pressure.¹² Hence, we can conclude that the change in monolayer structure observed above the pH window is not due to sodium hydroxide at high pH but due to a discrete change in the nature of the headgroup–cadmium ion interaction. Table 1 shows that A decreases and ξ increases when the pH rises above the window from the respective values within the window.

There are two possible processes which could account for the effect of pH on the interactions between the headgroups and ions. The first is that as the pH is raised, acid molecules are converted to soaps (salts). The fraction of cadmium soap to acid in transferred (LB) films has been found¹⁶ to increase linearly from 0 to 1 over the pH range 4.8–6.5. In our Langmuir monolayer, however, these values fall below the pH window where interactions between the headgroups and ions do not play a significant role. The process of deprotonation and conversion of acid to soap does not explain the structural changes at high pH that occur after the organic monolayer is saturated with the soap. The second possibility is that as the pH is raised, aqueous ions undergo hydrolysis and specific soluble hydroxide complexes may be formed. It is difficult to predict what particular hydroxide species of cadmium forms directly under the organic monolayer since the concentration and pH at the interface are unknown. However, it may be the interaction with a particular species of cadmium hydroxide complex (for example Cd₄(OH)₄⁴⁺(aq) which is dominant at high concentration of Cd²⁺(aq) and pH range 8–12)¹⁷ that forces the organic monolayer into a chiral structure. Different species of cadmium hydroxide dominate at different pH values,¹⁷ so the process of hydrolysis may explain the fact that the monolayer goes through a series of structures as the pH is raised.

The effects of increasing pH are both acid to soap conversion and hydrolysis. To study the effect of each process on the structure of the organic monolayer, we dissolved a comparatively large amount of sodium chloride in addition to cadmium chloride in the subphase and increased the pH to 9.3. Sodium monovalent cations might be expected to screen the negatively charged headgroups and reduce the ratio of acid to cadmium soap. We observed no change. The film was found in the same high pH phase as without sodium. Alkali group I elements do not hydrate well as opposed to cadmium which can form many hydrolysis products.¹⁷ This lends support to the possibility that there is a type of “hydration bridge” between the heads and cadmium ions within a specific pH range.

It is interesting to compare the effects of pH to the effects of temperature⁶ on the headgroup–ion interaction in Langmuir monolayers. In particular, we were interested in the effect of raising temperature on a monolayer within the pH window. Figure 5 shows the in-plane diffraction scans on a monolayer of C₂₁ acid with 10^{−4} M CdCl₂ in the subphase, the pH raised

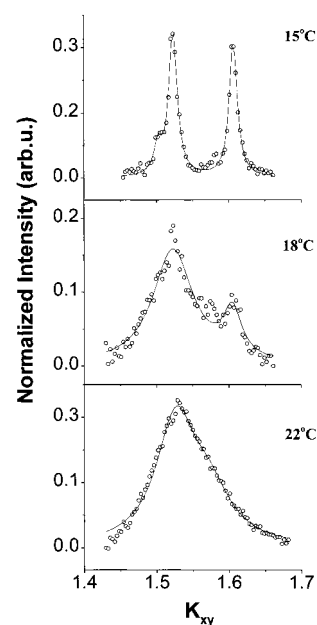


Figure 5. Normalized diffracted Intensity (arbitrary units) versus K_{xy} for a heneicosanoic acid Langmuir monolayer at pH ~ 8.5 and ~ 0 dyn/cm surface pressure, with 10^{−4} M CdCl₂ in the subphase and different temperatures. Data taken at $K_z = 0$.

TABLE 2: Changes in the Areas Per Headgroup and Per Chain^a

	pH (temp = 9.2 °C)			temp (pH = 8.5)		
	6.2	8.5	9.3	9.2 °C	18.0 °C	22.0 °C
ΔA (%)		−9.6	−11.32		0.11	0.95
$\Delta A'$ (%)		−3.6	−5.62		1.44	2.29

^a For pH, the change is with respect to pH ~ 6.2 . For temperature, the change is with respect to 9.2 °C.

to 8.5 by NaOH, pressure ~ 0 dyn/cm and temperatures ranging from 15 to 22 °C. The monolayer was found to be essentially unchanged from 9 to 15 °C, as is evident from a comparison of Figure 5 (top) (15 °C) with Figure 3 (middle) (9.2 °C). Along with this characteristic triplet we also found all the superlattice peaks at 15 °C (not shown in the figure). At 18 °C (Figure 5 (middle)) we found two broad, in-plane peaks and no peaks anywhere else. However, the data were not very reproducible at this temperature and we would sometimes start with a pattern as in Figure 5 (top) which changed rapidly, in subsequent scans, to the situation in Figure 5 (middle). This is probably due to hysteresis at a first-order transition.

At 22 °C, the monolayer exhibited a stable and reproducible diffraction pattern (Figure 5 (bottom)). Only one broad, asymmetric in-plane peak was observed over the whole region from 0.7 to 1.7 Å^{−1} (see Table 1). This structure is very similar to that of the high-temperature Rotator-I phase of pure C₂₁ monolayers at around 20 °C (ref 10). This phase is formed by a partial disorder in the orientations of the chain backbone planes.⁸ The effect of the cadmium ions is only to lower the effective temperature of the monolayer so that a monolayer with cadmium ions at 22 °C has the structure of a monolayer without the ions at 20 °C.

In order to understand better the effects of pH and temperature on the molecules in a monolayer we estimated the (percentile) changes in the area per headgroup (A) and area per chain (A') with increasing pH and increasing temperature. These changes are compared in Table 2. From this table we see that, with increase in pH, the reduction in area per headgroup is consider-

TABLE 3: Comparison of Structural Parameters with Different Ions in Subphase

salt	conc (M)	pH	temp (°C)	π (dyn/cm)	a (Å)	b (Å)	A (Å ²)	ξ	electronegativity
Zn(Ac) ₂	5×10^{-4}	5–7	10	~3	9.22	4.08	18.80	0.26	1.65
CdCl ₂	1×10^{-4}	>9	9.2	~0	7.45	5.00	18.64	0.15	1.69

ably more than the reduction in area per chain. This preferential reduction indicates that increase in pH acts as an attractive interaction and affects the headgroups more than the chains. On the other hand, when temperature is increased, the increase in area per headgroup is less than the increase in area per chain, indicating that temperature affects the chain–chain interactions more than it affects the headgroups. The fact that an increase of pH contracts and an increase of temperature expands the monolayer lattice contrasts with the case of monovalent cations, where the effect of raising pH was seen to be similar to that of raising temperature.⁶

2. Comparison with Zinc Ions. The nature of interaction of metal ions with acids is known to be correlated with the Pauling electronegativity of the metal.^{2,8,18} Metals with low electronegativity tend to form electrovalent bonds, i.e., interact through Coulomb attraction, while for metals with higher electronegativities the bond acquires an increasingly covalent character and the interaction becomes dominated by exchange forces. Cadmium is a metal with an intermediate value (1.69) on the Pauling electronegativity scale and it is expected to form partially covalent (polar) bonds with the headgroups in a fatty acid monolayer. The effect of only one other metal ion, calcium, on a fatty acid monolayer has been studied so far with GID.⁷ Calcium is a metal with a low electronegativity (1.00) and, on comparing the previous work on calcium with our results, we find that it affects the monolayer in a way similar to what is observed with cadmium ions above the pH window.

In order to gain a better correlation of the nature of headgroup–metal ion interactions with the electronegativity of the divalent metal, we performed GID studies on the effect of another divalent metal ion on C₂₁ acid monolayers under conditions similar to those for cadmium. We chose zinc which has the electronegativity value of 1.65, close to but less than the electronegativity value of cadmium, and belongs to the same group (IIB). Zinc is also interesting for its two somewhat anomalous properties. First, the area per molecule of zinc–fatty acid salts in LB films is too large to be correlated with its electronegativity.² Second, the first few monolayers have a hexatic structure before subsequent monolayers form the “bulk” crystal structure.¹⁹ The in-plane positional correlations were observed to be short-range, but with long-range bond-orientational order. Those observations suggest that the intermolecular interactions of fatty acid salts of zinc are much weaker than of salts of cadmium in LB films.

Figure 6a shows the scan for the monolayer with CdCl₂ in the subphase at pH ~ 9.3. Figure 6b shows the scan for the monolayer with Zn(Ac)₂ in the subphase at pH ~ 7.0, the maximum pH that can be reached before the monolayer becomes unstable, 10 °C, and the low pressure of ~3 dyn/cm. Only these two in-plane peaks were observed for the entire scan range of 0.6–1.7 Å⁻¹ and, except for slight shifts in the peak positions, no essential change in the diffraction pattern was observed in the pH range from ~5 to 7. What is more important is that there were no superlattice peaks at low K_z , and the observed peaks were always in-plane. Analysis of the data in Figure 6b gave the structure of the monolayer to be composed of centered rectangular cells (two molecules per cell) with untilted chains. The structural parameters are presented in Table 3.

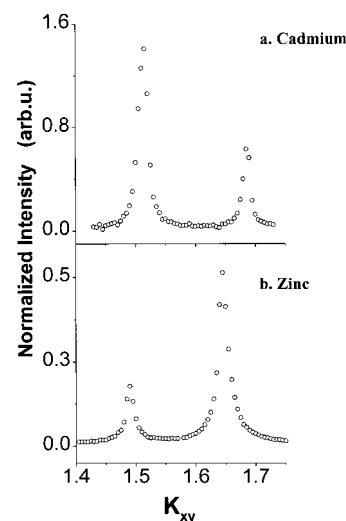


Figure 6. Normalized diffracted intensity (arbitrary units) versus K_{xy} for a heneicosanoic acid Langmuir monolayer with (a) 10^{-4} M CdCl₂ at ~9.2 °C and ~0 dyn/cm surface pressure, pH ~ 9.3; (b) 5×10^{-4} M Zn(Ac)₂ at ~10 °C and ~3 dyn/cm surface pressure, pH ~ 7.0.

The area per headgroup is only slightly smaller for a monolayer with cadmium than with zinc, but the lattice parameters are significantly different between the two ions. In general, parameters of the unit cell can vary such that the packing of hydrocarbon chains can be found between two modes of arrangement: herringbone (HB) and pseudoherringbone (PHB).⁸ The rectangular unit cell dimensions of $5.0 \text{ Å} \times 7.5 \text{ Å}$ for cadmium are a fingerprint of the HB pattern whereas the dimensions $4.1 \text{ Å} \times 9.2 \text{ Å}$ for zinc are close to that for PHB packing. The PHB packing mode has a lower packing density than that of the HB structure. The PHB packing mode of the monolayer with zinc, therefore, may explain the lower in-plane cohesion as well as lower packing density in LB films of zinc fatty acid salts as opposed to cadmium salts.

Table 3 also indicates that (a) the nature of headgroup–divalent ion interaction in a monolayer with cadmium ions in the subphase and above the pH window is similar to the interaction in a monolayer with zinc ions (with electronegativity value very close but lower than that of cadmium) in the subphase, under comparable external conditions; and (b) the strength of the attractive interaction, estimated from the area per headgroup, is lower for zinc than for cadmium.

Conclusions

Not all metal ions form lattices under Langmuir monolayers. Of the ions reported so far, only cadmium does so, and only in a narrow pH window (7–9). At lower pH, the cadmium ions have no effect on the monolayer; at higher pH, they isotropically compress the monolayer. Within this window the organic monolayer lattice becomes chiral and shows three first-order diffraction peaks, and there are other weak peaks at lower in-plane wave-vector magnitudes corresponding to an ordered superlattice.

Our studies, as well as ref 9, suggest that formation of the chiral phase of the fatty acid monolayer is closely related to the appearance of superlattice peaks. If the superlattice is due

to metal ions, the appearance of the chiral phase can act as an indicator of superlattice formation in cases of light (low-*Z*) metals, e.g. zinc. Since we could not see the monolayer chiral phase with zinc in the subphase, we expect that the superlattice does not form in this case.

Zinc has an electronegativity value very close to cadmium, and they belong to the same group (IIB) in the periodic table. Therefore, if the character of headgroup-ion interaction is at all correlated with electronegativity of the metal, there seems to be a sudden change in this interaction at or very close to the cadmium electronegativity value. Although we do not know what is special about cadmium and about this pH range, it is suggestive that the rod scans of the superlattice peaks indicate a film thickness of ~ 10 Å. Perhaps the superlattice is not a monolayer of cadmium ions, as has been assumed,⁹ but a layer of a larger ionic complex formed only in this pH window. As a matter of fact, the presence of an ionic complex was suggested from reflectivity studies of the fatty acid monolayer with cadmium ions in the subphase when the pH was raised by $\text{NH}_4\text{-OH}$, but no such complex was indicated from the reflectivity data when NaOH was used.⁹ Further studies, perhaps using spectroscopic techniques, will be necessary to probe the nature of the subphase region just under the monolayer.

Acknowledgment. This work was supported by the US Department of Energy under grant no. DE-FG02-84ER45125. This research was performed in part at Beam Line X14A of the National Synchrotron Light Source, Upton, NY: both the beam line and the synchrotron facility are supported by the US Department of Energy.

References and Notes

- (1) Schwartz, D. K. *Surf. Sci. Rep.* **1997**, 27, 241–334.
- (2) Zasadzinski, J. A.; Viswanathan, R.; Madsen, L.; Garnaes, J.; Schwartz, D. K. *Science* **1994**, 263, 1726.
- (3) Yazdani, M.; Yu H.; Zografi, G. *Langmuir* **1990**, 6, 1093.
- (4) Gericke, A.; Hühnerfuss, H. *Thin Solid Films* **1994**, 245, 74–82.
- (5) Ulman, A. *An Introduction to Ultrathin Organic Films from Langmuir–Blodgett to Self-Assembly*; Academic Press: New York, 1991.
- (6) Datta, A.; Kmetko, J.; Richter, A. G.; Yu, C.-J.; Dutta, P.; Chung, K.-S.; Bai, J.-M. *Langmuir* **2000**, 16, 1239.
- (7) Shih, M. C.; Bohanon, T. M.; Mikrut, J. M.; Zschack, P.; Dutta, P. *J. Chem. Phys.* **1992**, 96, 1556.
- (8) Kaganer, V. M.; Möhwald, H.; Dutta, P. *Rev. Mod. Phys.* **1999**, 71, 779.
- (9) Böhm, C.; Leveiller, F.; Jacquemain, D.; Möhwald, H.; Kjaer, K.; Als-Nielsen, J.; Weissbuch, I.; Leiserowitz, L. *Langmuir* **1994**, 10, 830.
- (10) Barton, S. W.; Thomas, B. N.; Rice, S. A.; Lin, B.; Peng, J. B.; Ketterson, J. B.; Dutta, P. *J. Chem. Phys.* **1988**, 89, 2257.
- (11) Vineyard, G. H. *Phys. Rev. B* **1982**, 8, 4146.
- (12) Durbin, M. K.; Malik, A.; Richter, A. G.; Ghaskadvi, R.; Gog, T.; Dutta, P. *J. Chem. Phys.* **1997**, 106, 8216.
- (13) Kaganer, V. M.; Peterson, I. R.; Kenn, R. M.; Shih, M. C.; Durbin, M.; Dutta, P. *J. Chem. Phys.* **1995**, 102, 9412.
- (14) Small, D. M. *The Physical Chemistry of Lipids, Handbook of Lipid Research*; Plenum Press: New York, 1986; Vol. 4, p 611.
- (15) Shih, M. C.; Bohanon, T. M.; Mikrut, J. M.; Zschack, P.; Dutta, P. *Phys. Rev. A* **1992**, 45, 5734.
- (16) Petrov J. G.; Kuleff, I.; Platikanov D. *J. Coll. Interface Sci.* **1982**, 88, 29.
- (17) Baes, C. F.; Mesmer, R. E. *The Hydrolysis of Cations*; Wiley: New York, 1976.
- (18) Pauling, L. *The Nature of the Chemical Bond*; Cornell University Press: New York, 1960.
- (19) Viswanathan, R.; Madsen, L. L.; Zasadzinski, J. A.; Schwartz, D. K. *Science* **1995**, 269, 51.